Check for updates

The Journal of Phytopharmacology 2025; 14(3):188-202
Online at: www.phytopharmajournal.com

Research Article

ISSN 2320-480X
JPHYTO 2025; 14(3): 188-202
May- June
Received: 04-05-2025
Accepted: 12-07-2025
Published: 31-07-2025

doi: 10.31254/phyto.2025.14310

Olubusola Omobolanle Olaleye
1. School of Pharmacy, University of Nottingham, University Park Campus, Nottingham, NG7 2RD, United Kingdom
2. Centre for Analytical Bioscience, Advanced Materials & Healthcare Technologies Division, School of Pharmacy, University of Nottingham, Nottingham, NG7 2RD, United Kingdom
3. Department of Pharmacognosy, Faculty of Pharmacy, College of Medicine Campus, University of Lagos, Lagos State, Nigeria

Dong-Hyun Kim
1. School of Pharmacy, University of Nottingham, University Park Campus, Nottingham, NG7 2RD, United Kingdom
2. Centre for Analytical Bioscience, Advanced Materials & Healthcare Technologies Division, School of Pharmacy, University of Nottingham, Nottingham, NG7 2RD, United Kingdom

Keith A Spriggs
School of Pharmacy, University of Nottingham, University Park Campus, Nottingham, NG7 2RD, United Kingdom

Correspondence:
Dr. Olubusola Omobolanle Olaleye
Department of Pharmacognosy, Faculty of Pharmacy, College of Medicine Campus, University of Lagos, University Rd, Lagos, P.M.B. 12003, Nigeria
Email: olu-olaleye@unilag.edu.ng

Evaluation of anticancer activity and phytochemical characterisation of *Musanga cecropioides* R. Br. ex Tedlie (Urticaceae) leaf extract

Olubusola Omobolanle Olaleye, Dong-Hyun Kim, Keith A Spriggs

ABSTRACT

Background: Cancer remains a leading global health challenge, accounting for approximately 10 million deaths annually. While conventional treatments such as surgery, chemotherapy, and radiotherapy are widely used, medicinal plants offer promising alternatives due to their bioactive constituents. *Musanga cecropioides* R. Br. ex Tedlie (Urticaceae), a plant native to West Africa, has been traditionally used for various ailments but remains underexplored for its anticancer potential. **Objective:** This study aimed to evaluate the anticancer activity of *Musanga cecropioides* leaf (MCL) extract against breast cancer cell lines MCF-7 and MDA-MB-231, elucidate its mechanisms of action, and identify bioactive compounds responsible for its cytotoxic effects. **Materials and Methods:** Ethanol extract of MCL was prepared and tested on MCF-7, MDA-MB-231, and non-cancer MRC-5 cells using the MTT assay to determine cell viability and selectivity. Flow cytometry was employed to assess cell cycle progression, apoptosis (Annexin V-FITC/PI), and DNA damage (γ-H2AX assay). Caspase-3/7 activation and reactive oxygen species (ROS) generation were measured using chemiluminescence assays. Bioassay-guided fractionation was performed using solvent partitioning and chromatographic techniques. Structural elucidation of the isolated compounds was conducted using ultraviolet-visible light spectroscopy (UV), infrared spectroscopy (IR), nuclear magnetic resonance (NMR), and liquid chromatography coupled with mass spectrometry (LC-MS). **Results:** MCL extract inhibited proliferation of MCF-7 and MDA-MB-231 cells with GI_{50} values of 3.42±1.80 µg/mL and 24.59±3.33 µg/mL, respectively, showing selectivity over non-cancer lung fibroblasts, MRC-5 cells. Flow cytometry revealed G1 phase arrest in MCF-7 cells and possible G2/M arrest in MDA-MB-231 cells. Apoptosis was induced in both cell lines, with caspase-3/7 activation observed in MDA-MB-231 but not in MCF-7 cells. ROS generation and DNA double-strand breaks were significantly elevated in treated cells. Bioassay-guided fractionation yielded 28 compounds, with docosanoic acid and α-tocopherol identified as major bioactive constituents. **Conclusion:** *Musanga cecropioides* leaf extract exhibits potent and selective anticancer activity against breast cancer cells through mechanisms involving cell cycle arrest, apoptosis induction, ROS generation, and DNA damage. The identification of docosanoic acid and α-tocopherol supports its potential as a source of chemotherapeutic agents, warranting further preclinical investigation.

Keywords: Breast cancer, Anticancer activity, Apoptosis induction, Bioassay-guided fractionation.

INTRODUCTION

Cancer is the second leading cause of mortality worldwide with the number of cancer-related fatalities increasing daily [1]. Surgery, chemotherapy and irradiation are the commonest treatment choices [2]. Natural products have been a major source of innovative anticancer therapies due to their inherent biological activity, which has allowed the development of chemical entities demonstrating both safety and efficacy [3]. Exploring medicinal plants for bioactive constituents may provide fresh perspectives for innovative drug discovery and development [4]. Nigeria has a rich biodiversity of indigenous plants utilised in herbal medicine to treat ailments and injuries, many of which have not yet been fully explored for their therapeutic potential [5].

People have been using plants as medicine for many years, and some contemporary medications have been extracted from them based on their traditional use, phytochemical analyses, and pharmacological assessments [6]. Extracts obtained from these plants contain a combination of natural products which requires a series of purification steps for the isolation of the bioactive components [7]. Bioassay-guided fractionation is an efficient method for separating chemical constituents with good biological activity [8]. Utilising various separation techniques such as thin layer chromatography (TLC), column chromatography, gas chromatography, and high-performance liquid chromatography (HPLC), bioactive natural compounds have been purified and identified [9]. Amongst all these techniques, column chromatography and thin-layer chromatography (TLC) are widely used owing to their affordability,

ease of use, and availability in a variety of stationary phases such as silica gel and alumina [10]. Data from a variety of spectroscopic methods, including ultraviolet-visible light (UV), infrared (IR), nuclear magnetic resonance (NMR), and mass spectrometry, are used to determine the structure of natural products [11].

Musanga cecropioides R. Br. ex Tedlie, Urticaceae, is an evergreen plant that grows up to 30 m tall forming an umbrella-like cover [12]. In some African countries, including Angola, Cameroon, Ghana, and Nigeria, different parts of the plant are employed in ethnomedicine to treat inflammation, abscess, dysmenorrhea, hypertension, oedema, gonorrhea, and wounds [13]. Our previous study demonstrated the antiproliferative activity of the leaf and stem extracts of the plant amongst others against a panel of human cancer cell lines, including ovarian (HeLa), liver (HUH-7) and breast (MCF-7 and MDA-MB-231) [14]. This study was therefore aimed at investigating the anticancer activity of *Musanga cecropioides* leaf (MCL) extract in a bid to identify the mechanisms by which MCL extract exerts growth-inhibitory effects in breast cancer cell lines, including MCF-7 and MDA-MB-231 cells and to characterise some of the bioactive components in the extract.

MATERIALS AND METHODS

Chemicals and solvents

Dimethyl sulfoxide (DMSO), trypsin 10X, phosphate-buffered saline (PBS), heat-inactivated foetal bovine serum (FBS), and standard compounds (quercetin, docosanoic acid, and α-tocopherol) were obtained from Sigma-Aldrich (St. Louis, MO, USA). Chromatographic-grade methanol, butanol, ethyl acetate, dichloromethane, and n-hexane were sourced from Thermo Fisher Scientific, UK. All chemicals and reagents used were of analytical, biological, or molecular biology grade.

Plant collection and authentication

Fresh leaves of *M. cecropioides* were collected in February 2021 from Oru Ijebu, Ogun State (Latitude: 6.9526° N, Longitude: 3.9434° E) with permission from the Forestry Research Institute of Nigeria (FRIN). The plant was identified and authenticated by Chukwuma Emmanuel of the same institute, and an herbarium specimen was deposited at the Forestry Herbarium Ibadan (FHI) with an assigned accession number.

Preparation of ethanol extract from *M. cecropioides* leaves

Fresh leaves were dried at room temperature under shade for 2 weeks, then pulverized using a Christy and Morris 8** Lab Mill. The 3.9 kg crushed sample was extracted with 96% ethanol for 72 hours, filtered through Whatman No. 1 paper, and concentrated using a Buchi Rota-vapor R205 (Brinkman, Switzerland) rotary evaporator at 40 °C.

Cell culture

MCF-7 and MDA-MB-231 human breast cancer cells were obtained from ATCC (Manassas, USA), while MRC-5 non-cancer lung fibroblasts were provided by Dr Tracey Bradshaw (University of Nottingham). Breast cancer cells were cultured in DMEM with 2 mM L-glutamine and 10% FBS, and MRC-5 cells in MEM supplemented with 10% FBS, L-glutamine, non-essential amino acids, and 1 mM HEPES, at 37 °C in 5% CO_2. Cell lines were sub-cultured twice weekly to maintain logarithmic growth. They were also tested to ensure they were free of mycoplasma contamination.

Preparation of ethanol extract from *M. cecropioides* leaves

MCL extract (100 mg) was dissolved in 1 mL DMSO to make a 100 mg/mL stock solution, filtered through a 0.20 µm sterile filter. A 1000 µg/mL working solution was prepared in DMEM or MEM and serially diluted two-fold to achieve test concentrations of 1.95–250 µg/mL, with DMSO content kept below 1% in all cases.

Cell viability assay (MTT assay) and selectivity index study

Cell viability was assessed using the [3-(4,5-dimethylthiazol-2-yl)-2,5- diphenyl tetrazolium bromide (MTT) assay to measure mitochondrial succinate dehydrogenase activity. Our previously reported protocol for MTT assay as well as selectivity index study was adopted [14].

Cell cycle analysis

Cell cycle analysis was performed via flow cytometry using propidium iodide (PI) staining (Sigma-Aldrich, USA). MCF-7 and MDA-MB-231 cells (5×10^4 /well) were plated in 6-well plates and allowed to adhere for 24 h. Cells were treated with MCL extract at 0.5×GI_{50}, 1×GI_{50}, and 2×GI_{50} concentrations, with 0.1% DMSO as a negative control and 2 µM etoposide as a positive control, followed by 72 h incubation. Floating and attached cells were collected, washed with PBS, fixed in 70% ethanol overnight at 4°C, and stained with a fluorochrome solution containing PI, RNAse, Triton X-100, and sodium citrate at 37°C for 15 min [15]. Data were acquired using a Beckman Coulter flow cytometer (Brea, CA, USA), and analysis was performed in triplicates using Kaluza software version 2.1.00002.20011.

FITC Annexin V/PI apoptosis detection

Apoptotic cells were detected using the Annexin V-FITC apoptosis detection kit (Invitrogen, USA) per the manufacturer's protocol. MCF-7 and MDA-MB-231 cells (5×10^4 /well) were seeded in 6-well plates, allowed to adhere for 24 h, and treated with MCL extract at 0.5×GI_{50}, 1×GI_{50}, and 2×GI_{50} for 72 h. Controls included 0.1% DMSO (negative) and 2 µM etoposide (positive). Adherent and floating cells were collected, washed with PBS, centrifuged, and stained with 5 µL Annexin V-FITC and 150 µL binding buffer. After incubation in the dark for 15 min, 10 µL propidium iodide (50 µg/mL) and 400 µL binding buffer were added. Flow cytometry analysis (Beckman Coulter, Brea, CA, USA) was performed within 1 h, acquiring 20,000 events per sample. Data were analysed using Kaluza software, generating annexin V-FITC vs. PI fluorescence dot plots [16].

Assessment of DNA damage (γ-H2AX assay)

Cells (1×10^6) were seeded in 10 cm^2 dishes and incubated at 37°C with 5% CO_2 for 24 h to adhere. They were then treated with test agents at 0.5×GI_{50}, 1×GI_{50}, and 2×GI_{50} for 24 h, with 0.1% DMSO as a negative control and 2 µM etoposide as a positive control. Floating and adherent cells were collected, fixed in 4% formaldehyde for 5 min, and permeabilized with 0.4% Triton X-100 in PBS. After washing, cells were incubated with 200 µL of H2AX antibody (1:3333) for 1.5 h, followed by 200 µL of goat anti-mouse Alexa Fluor™ antibody (1:1750) for 1 h in the dark. Finally, cells were stained with PI/RNAse solution and analysed using a Beckman Coulter flow cytometer and Kaluza software [17].

Caspase-3/7 activation assay

Caspase-3/7 activation was assessed using the Caspase-Glo® 3/7 assay kit (Promega, USA). Cells (5×10^3/well) were seeded in white 96-well plates and incubated for 24 h at 37°C with 5% CO_2. They were treated with MCL extract at 1×GI_{50} for 24 h. Caspase-Glo 3/7 reagent was then added in a 1:1 ratio with the culture medium, mixed for 30 sec, and incubated for 1 h at room temperature in the dark. Luminescence was measured using the GloMax-Multi Detection System (Promega, USA) [18].

Detection of reactive oxygen species

Cells (5×10^3/well) were seeded in white 96-well plates with 100 µL of culture medium and incubated for 24 h at 37°C with 5% CO_2. Afterward, the medium was replaced with 80 µL of MCL extract at 1×GI_{50} for 24 h. Six hours before the end of incubation, 20 µL of 125 µM chilled H_2O_2 substrate buffer was added. Following incubation, 100 µL of ROS-Glo™ detection solution was added, including 10 µL each of d-Cysteine and Signal Enhancer Solution per 1 mL of luciferin reagent. After 20 min at room temperature, luminescence was measured using the GloMax-Multi Detection System (Promega, USA).

Fractionation of MCL extract and bioactivity of fractions

A 300 g crude extract was dissolved in 400 mL distilled water and partitioned with n-hexane, dichloromethane (DCM), ethyl acetate (EA), and n-butanol in increasing polarity (500 mL × 5 for each, except BuOH: 500 mL × 3). Fractions (Hex, DCM, EA, BuOH, and AQ) were concentrated using a rotary evaporator (Buchi, Switzerland) and stored at 4°C. Growth inhibitory activities were evaluated on MCF-7 cells using the MTT assay and fractions with the lowest GI_{50} values were identified as active.

Purification of fractions and column chromatography

The DCM and ethyl acetate fractions were subjected to normal-phase column chromatography (CC) using a silica gel 60 column (2.5 cm × 20 cm) (230-400 mesh, Merck, Germany). Samples were eluted with solvent gradients of hexane:ethyl acetate (100:0 to 0:100), ethyl acetate:methanol (100:0 to 0:100), and 100% methanol to produce sub-fractions. Eluents (20 mL each) were monitored via TLC, and fractions with similar Rf values were combined. Preparative TLC was used for purification by loading samples onto glass plates, developing them in appropriate mobile phases, and viewing under UV light. Isolated compounds were extracted with DCM and methanol, evaporated under reduced pressure at 40°C, and analysed under UV light and with detection reagents (vanillin-sulphuric acid, iodine, and potassium permanganate) to confirm purity.

Nuclear magnetic resonance (NMR) spectroscopy

Tetramethylsilane (TMS) was used as an internal standard, and deuterated chloroform ($CDCl_3$) was used to dissolve samples (5-15 mg) for NMR analysis on a Bruker NMR (500 MHz). Samples were vacuum-dried to remove water, dissolved in 650 µL $CDCl_3$, filtered, and placed in a pp535 NMR tube. 1D NMR, ^1H (proton NMR) and ^{13}C (carbon NMR) along with 2D NMR, Heteronuclear Single Quantum Coherence (HSQC) and Distortion less Enhancement by Polarisation Transfer (DEPT 135) data were collected and analysed using MestReNOVA x64-12.0.4-22023 software.

Fourier Transform Infrared (FT-IR) spectroscopic analysis

The functional groups of spots were identified using FTIR spectroscopy. ATR with a dial path accessory (Agilent Cary 630 FTIR) was used to collect spectra in the 4000-650 cm^{-1} range at room temperature. Samples in $CDCl_3$ were scanned by applying steady pressure to a drop placed on the germanium component, with background absorption and $CDCl_3$ spectra also recorded. Data were analysed using MicroLab Expert FTIR software.

Liquid chromatography-Mass Spectrometry (LC-MS)

LC-MS analysis of isolated spots was performed using a Dionex UltiMate 3000 RS system coupled with a Q-Exactive Plus mass spectrometer (Thermo Fisher Scientific) following the protocol of (19). The MS was operated in ESI+ and ESI− modes with tandem MS at 30 eV (or higher where necessary). Calibration was done with positive (m/z +195) and negative (m/z -265) standards. A reversed-phase ACE Excel 2 SuperC18 column (50 x 2.1 mm, 2 µm) was used for separation with a 10 µL injection at 300 µL/min for 15 min, with mobile phase gradients from 30% B to 100% B. Ion source parameters were set for positive and negative ionisation modes. Full MS scans (m/z 70-1050) were recorded with 50,000 resolutions. Data analysis was conducted using X-Calibur software version 4.0 (Thermo Fisher Scientific, Hemel Hempstead, UK). Putative identification of compounds was performed using Compound Discoverer software version 3.3 SP1.

Statistical analyses

Data were analysed using GraphPad Prism 9.5.1 and presented as mean ± SD. Significant differences were determined by one-way ANOVA with Dunnet's test or two-way ANOVA with Tukey's test, as appropriate. Significance was defined as $p < 0.05$, $p < 0.01$, $p < 0.001$, and $p < 0.0001$. All tests were performed in triplicate (n = 3), unless otherwise stated.

RESULTS

To gain mechanistic insights into MCL-induced growth inhibition in MCF-7 cells earlier reported (GI_{50} concentration = 3.42±1.80 µg/mL) [14], the growth-inhibitory activity of the extract on MDA-MB-231 along with normal (MRC-5) cells was evaluated by MTT assay. According to the International Agency for Research on Cancer (IARC), lung, breast, and prostate cancers have the highest occurrences worldwide [20]. Triple-negative breast cancer accounts for 10-15% of all breast cancers, having high reoccurrence rates. Furthermore, considering the biological variability of triple-negative breast cancer (TNBC), developing new medicines to tackle them is quite challenging. To this end, there is an urgent need to identify innovative potential treatments that are not only effective but also possess fewer undesirable side effects. From the results, the extract inhibited the growth of MDA-MB-231 cells with GI_{50} concentration of 24.59±3.33 µg/mL. The assay also revealed that MCL extract showed two-fold selectivity towards MDA-MB-231 cells compared with the non-cancer MRC-5 cells.

To investigate the involvement of cell cycle arrest as a potential mechanism by which MCL extract causes cell growth inhibition in MCF-7 and MDA-MB-231, cell cycle was assessed using flow cytometry. In MCF-7 cells, MCL extract caused a significant increase ($p<0.0001$) in the G1 phase cell population accompanied by a decrease in S and G2/M phases compared with control. The percentage of cell populations at G1 phase were 65.61 ± 0.91%, 71.70 ± 0.65% and 77.55 ± 2.05% at 0.5 x GI_{50} (1.71 µg/mL), 1 x GI_{50} (3.42 µg/ mL), and 2 x GI_{50} (6.84 µg/ mL), compared with control (58.41 ± 1.58%) (Figure 1). On the Other hand, with MDA-MB-231 cells, there was a significant drop in the G1 phase cell population which was accompanied by an increase in G2/M phase population in extract-treated cells at 0.5 x GI_{50} (12.30 µg/mL), 1 x GI_{50} (24.59 µg/mL) and 2 x GI_{50} (49.18 µg/mL) corresponding to 43.91±1.08, 40.80±0.57, and 40.35±0.28% respectively compared with control (36.46±1.81%) which was however not significant. This result suggests that MCL extract caused G1 phase cell cycle arrest in MCF-7 cells and possibly G2/M phase arrest in MD MB 231 cells (Figure 2). Supplementary file Figures S1 and S2 also show representative histograms of the dot plot of the cell cycle distribution in the two cell lines after treatment with MCL extract.

Using Annexin V-FITC/PI double labelling, it was further investigated if the antiproliferative effects of MCL extract on MCF-7 and MDA-MB-231 cells were connected to apoptosis induction. As illustrated in Figure 3, MCF-7 cells underwent apoptosis after 72 h wherein the extract exposure significantly increased ($p<0.0001$) late apoptotic cell population in a dose-dependent manner at concentrations of 0.5 x GI_{50} (1.71 µg/mL), 1 x GI_{50} (3.42 µg/mL), and 2 x GI_{50} (6.84 µg/mL) corresponding to 21.37±2.04%, 25.22±1.94% and 40.72±3.22%, respectively, compared with control 1.17±0.41%. Similarly, MDA-MB-231-treated cells exhibited a significant dose-dependent increase ($p<0.0001$) in the late apoptotic cell population at concentrations of (0.5 x GI_{50} (12.30 µg/mL), 1 x GI_{50} (24.59 µg/mL), and 2 x GI_{50} (49.18 µg/mL), corresponding to (5.33±0.11%,

6.56±0.33% and 8.54±2.12%, respectively), compared with control (0.06±0.03%) (Figure 4). The result from this study suggests that the cytotoxic activities displayed by MCL extract could be attributed to apoptotic and necrotic forms of cell death. Supplementary data Figures S3 and S4 also show representative dot plot of the apoptotic cell cycle distribution in the two cell lines after treatment with MCL extract.

To investigate the role of caspases in MCL-induced apoptosis in MCF-7 and MDA-MB-231 cells, the *in vitro* caspase activity assay was performed. The cells were treated with MCL extract at 1 x GI_{50} for 24 h and analysed by chemiluminescent assay to detect the activity of caspase 3/7. In MCF-7 cells, MCL extract did not significantly increase caspase activity (107.12±5.13% vs control) suggesting that caspase activation is not important in the MCL apoptosis-inducing ability in MCF-7 cells (Figure 5A). In MDA-MB-231 cells, MCL extract significantly elevated the activity of caspase 3/7 by 134.64±1.34% ($p<0.01$) (Figure 5B). This result implies that caspases play a role in the induction of apoptosis by MCL extract in MDA-MB-231 cells.

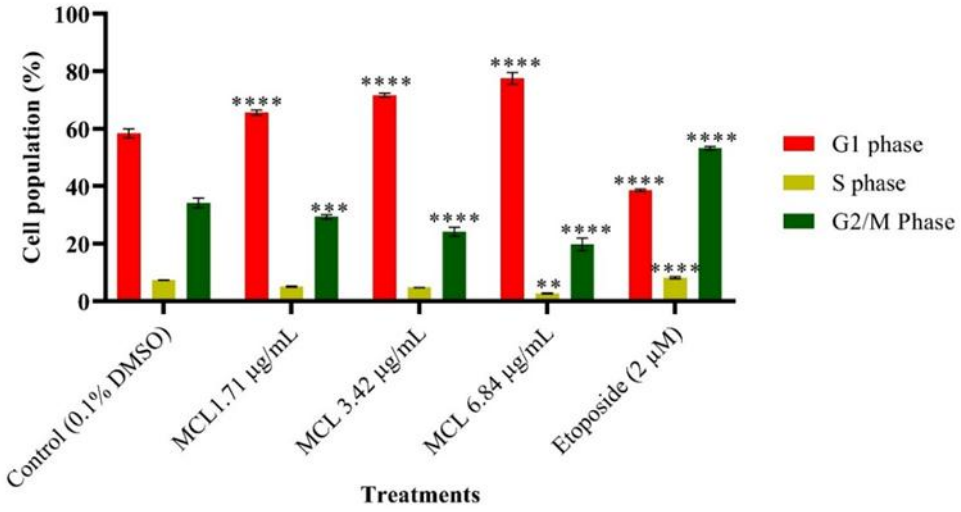

Figure 1: MCL causes GI phase arrest in MCF-7 cells after 72 h at all tested concentrations.

Results are presented as mean ± SD. Asterisks indicate significant p values **** $p < 0.0001$, *** $p < 0.001$, ** $p < 0.01$ vs. control Tukey's *post hoc* multiple comparison tests after a two-way ANOVA obtained from three separate studies (n=3).

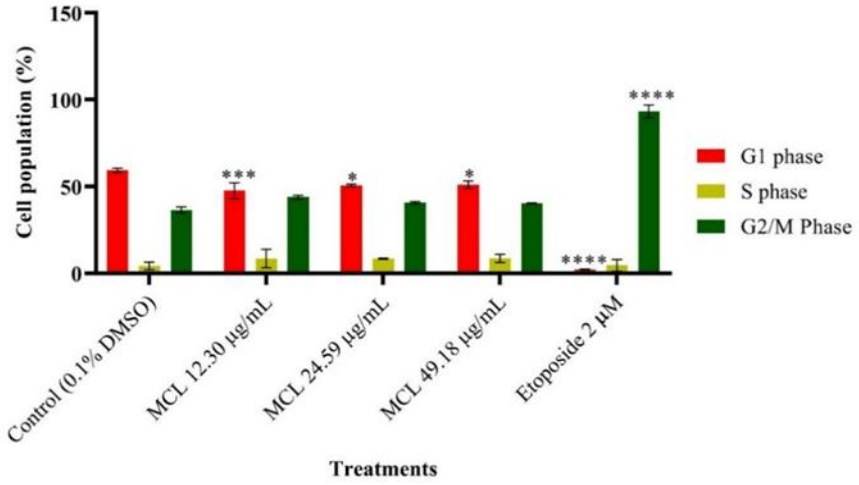

Figure 2: MCL shows possible G2/M phase cell cycle arrest in MDA-MB-231 after 72 h.

Results are presented as mean ± SD. Asterisks indicate significant p values * $p < 0.05$, *** $p < 0.001$, **** $p < 0.0001$ vs. control. Tukey's *post hoc* multiple comparison tests after a two-way ANOVA were obtained from three separate studies (n=3).

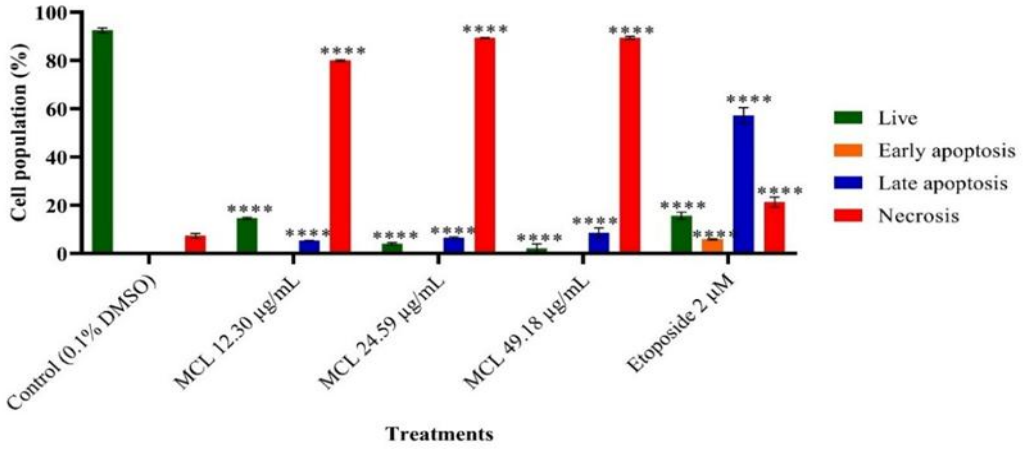

Figure 3: MCL extract induces apoptosis in MCF cells after 72 h

Results are presented as mean ± SD. Asterisks indicate significant p values ****p < 0.0001, ***p < 0.001, **p < 0.01, *p < 0.05 versus control. Tukey's *post hoc* multiple comparison tests after a two-way ANOVA were obtained from three separate studies (n=3).

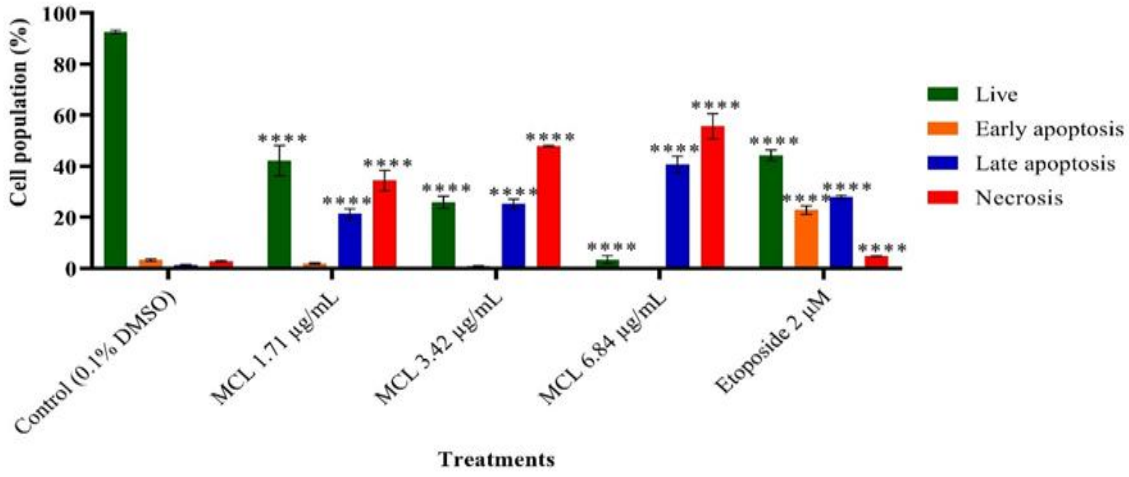

Figure 4: MCL extract induces apoptosis in MDA-MB-231 cells after 72 h

Results are presented as mean ± SD. Asterisks indicate significant p values ****p < 0.0001, ***p < 0.001, **p < 0.01, *p < 0.05 versus control. Tukey's *post hoc* multiple comparison tests after a two-way ANOVA obtained from three separate studies (n=3).

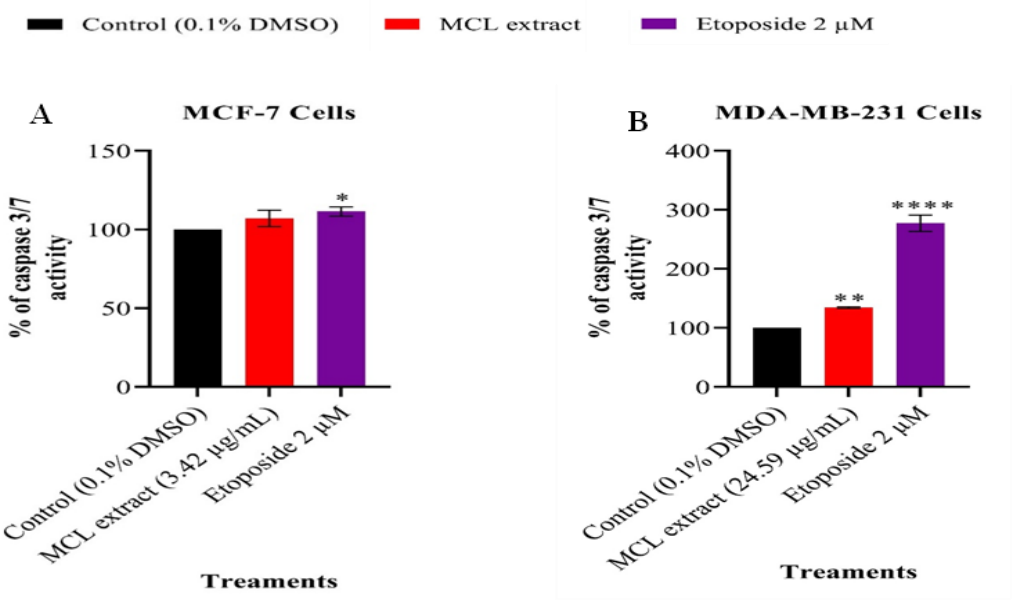

Figure 5: Effect of MCL extract on caspase 3/7 activity in MCF-7 (A) and MDA-MB-231 cells (B) Cells were treated with test agents at 1 x GI_{50} and analysed after 24 h exposure

Results are presented as mean ± SD. Asterisks indicate significant p values ****p < 0.0001, ***p < 0.001, **p < 0.01, *p < 0.05 versus control. Tukey's *post hoc* multiple comparison tests after a two-way ANOVA obtained from three separate studies (n=3).

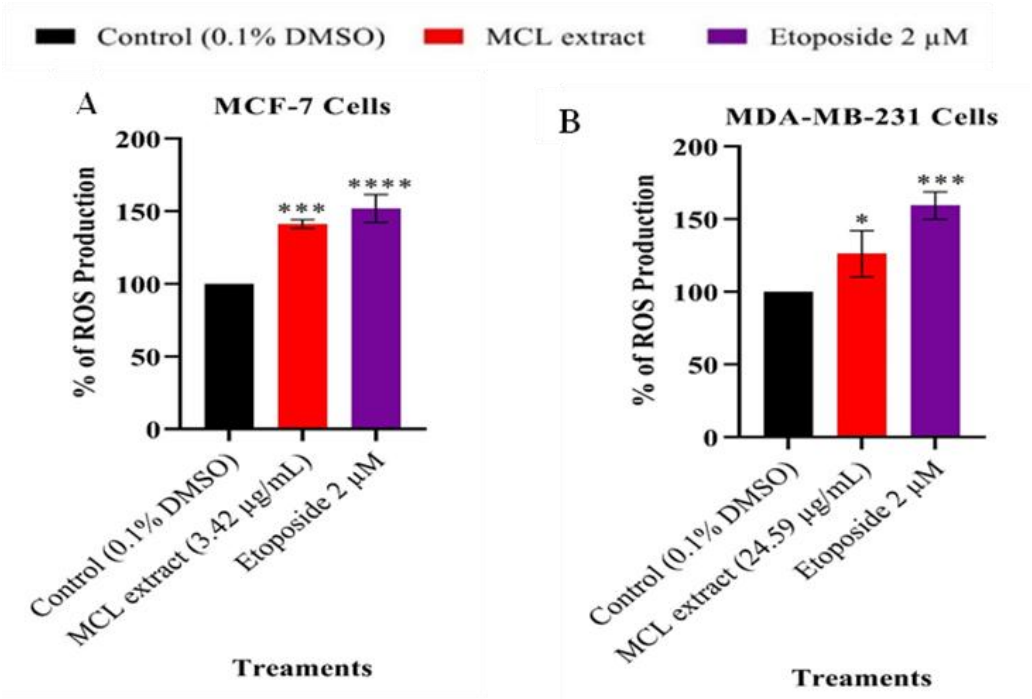

Figure 6: MCL extract induces ROS production in MCF-7 (A) and MDA-MB-231 cells (B) at 1 x GI_{50} after 24 h treatment.

Results are presented as mean ± SD. Asterisks indicate significant p values *p<0.05, ***p<0.001 and ****p<0.0001 versus control. Dunnet's *post hoc* multiple comparison tests after a one-way ANOVA obtained from three separate studies (n=3).

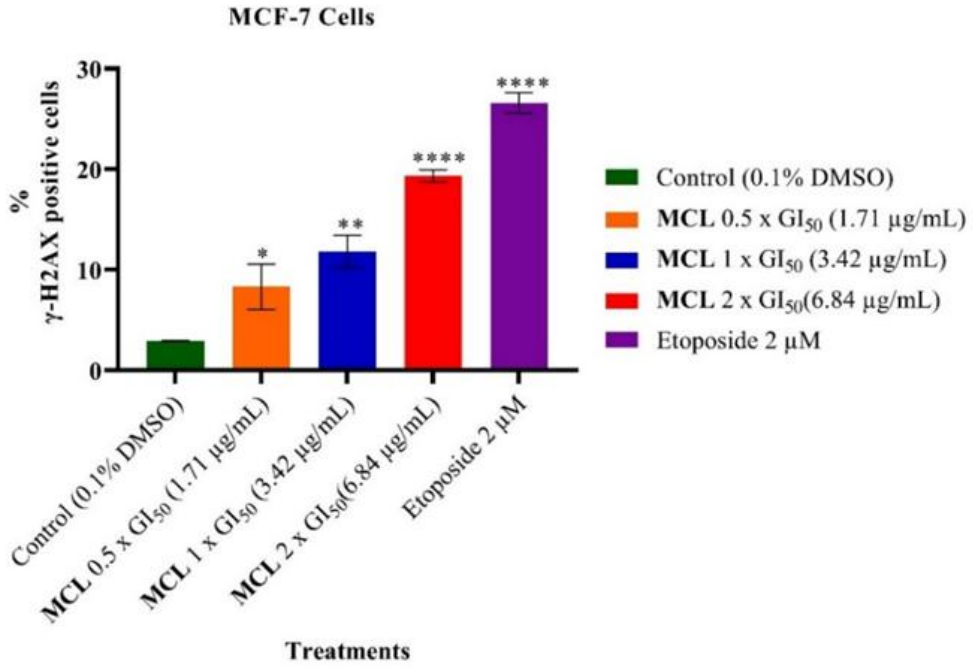

Figure 7a: MCL extract γ-H2AX in MCF-7 cells after 24 h exposure period.

Results are presented as mean ± SD. Asterisks indicate significant p values *p<0.05, **p<0.01, and ****p<0.0001 versus control using Dunnet's *post hoc* multiple comparison tests after a one-way ANOVA obtained from three separate studies (n=3).

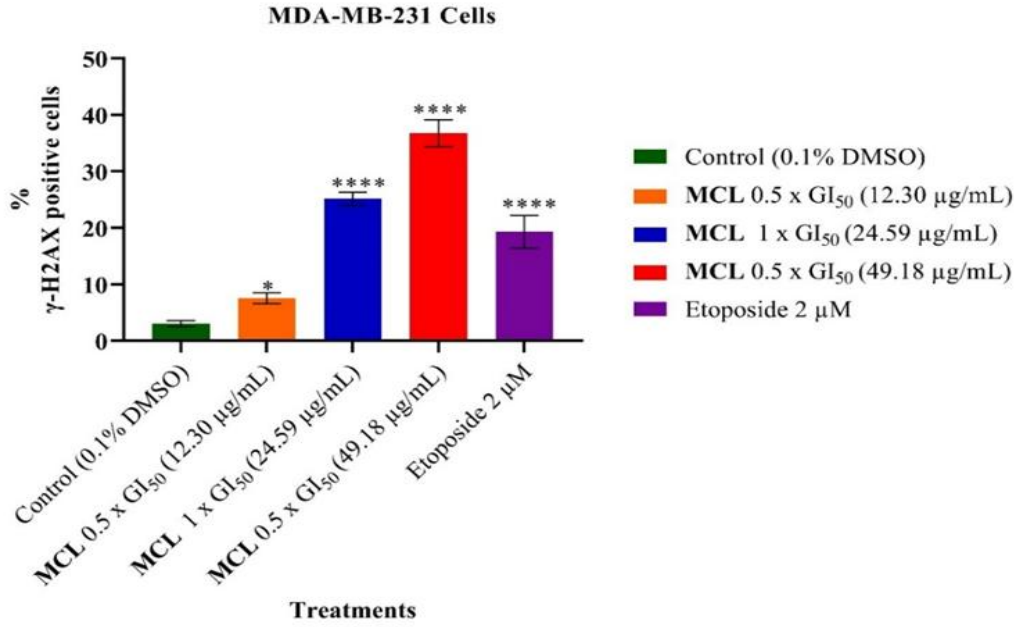

Figure 7b: MCL extract induces DSBs in MDA-MB-231 cells after 24 h treatment period.

Results are presented as mean ± SD. Asterisks indicate significant p values *p<0.05 and ****p<0.0001 versus control using Dunnet's *post hoc* multiple comparison tests after a one-way ANOVA obtained from three separate studies (n=3).

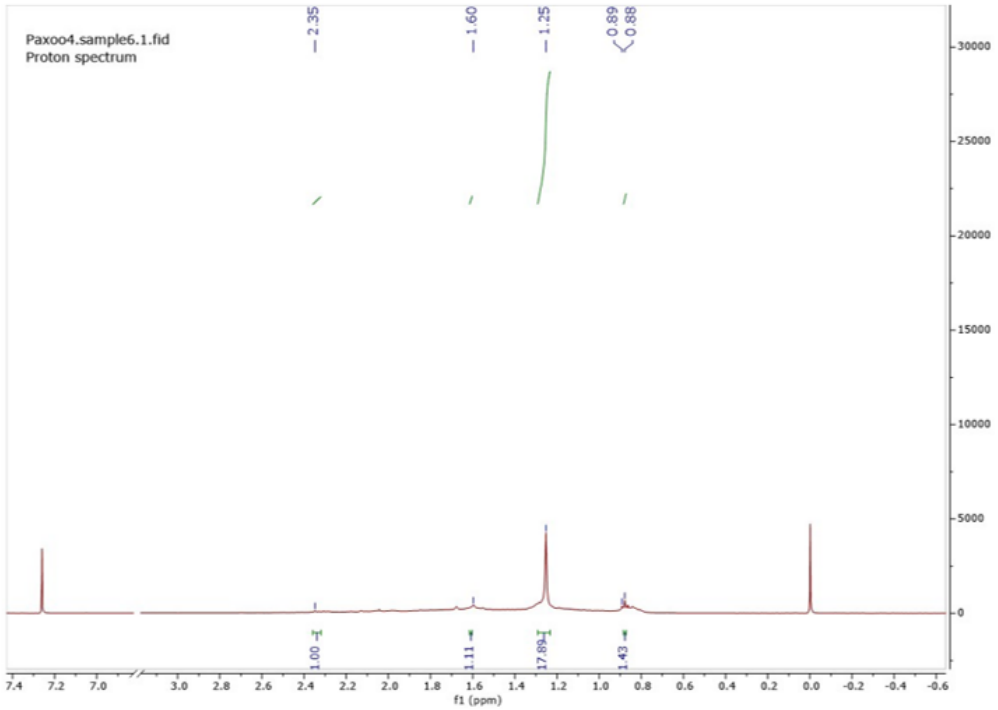

A

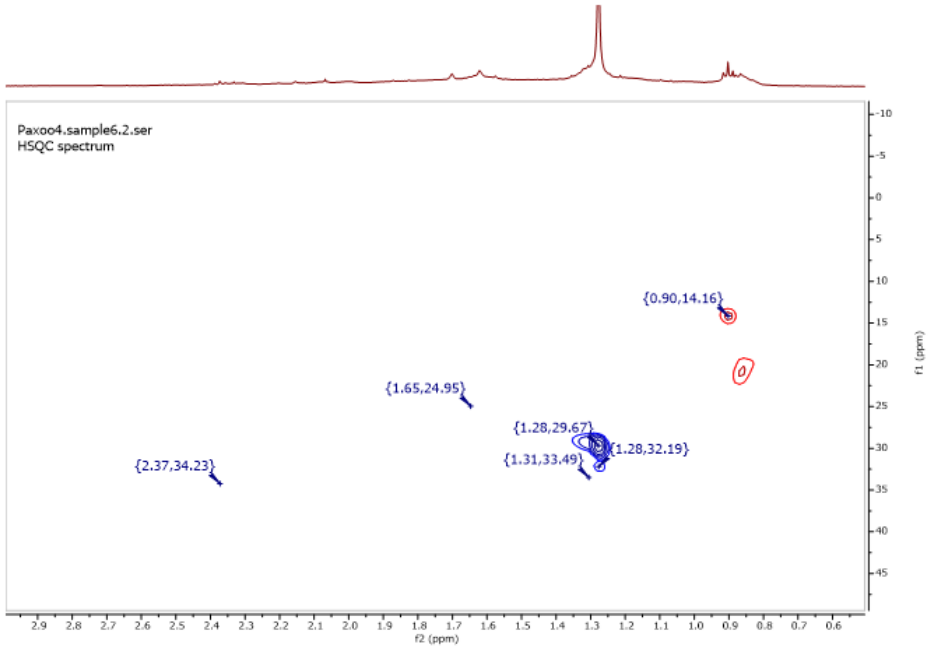

B

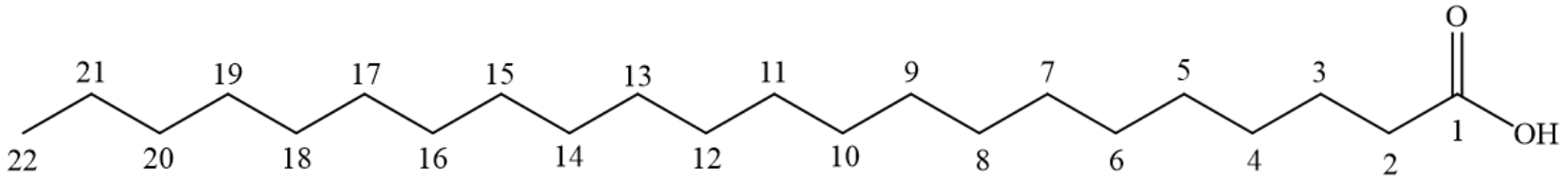

C

Figure 8a: ^{1}H NMR (A), HSQC (B) spectra and chemical structure of spot **6** (docosanoic acid, $C_{22}H_{44}O_2$) (C) isolated from *M. cecropioides* leaf extract

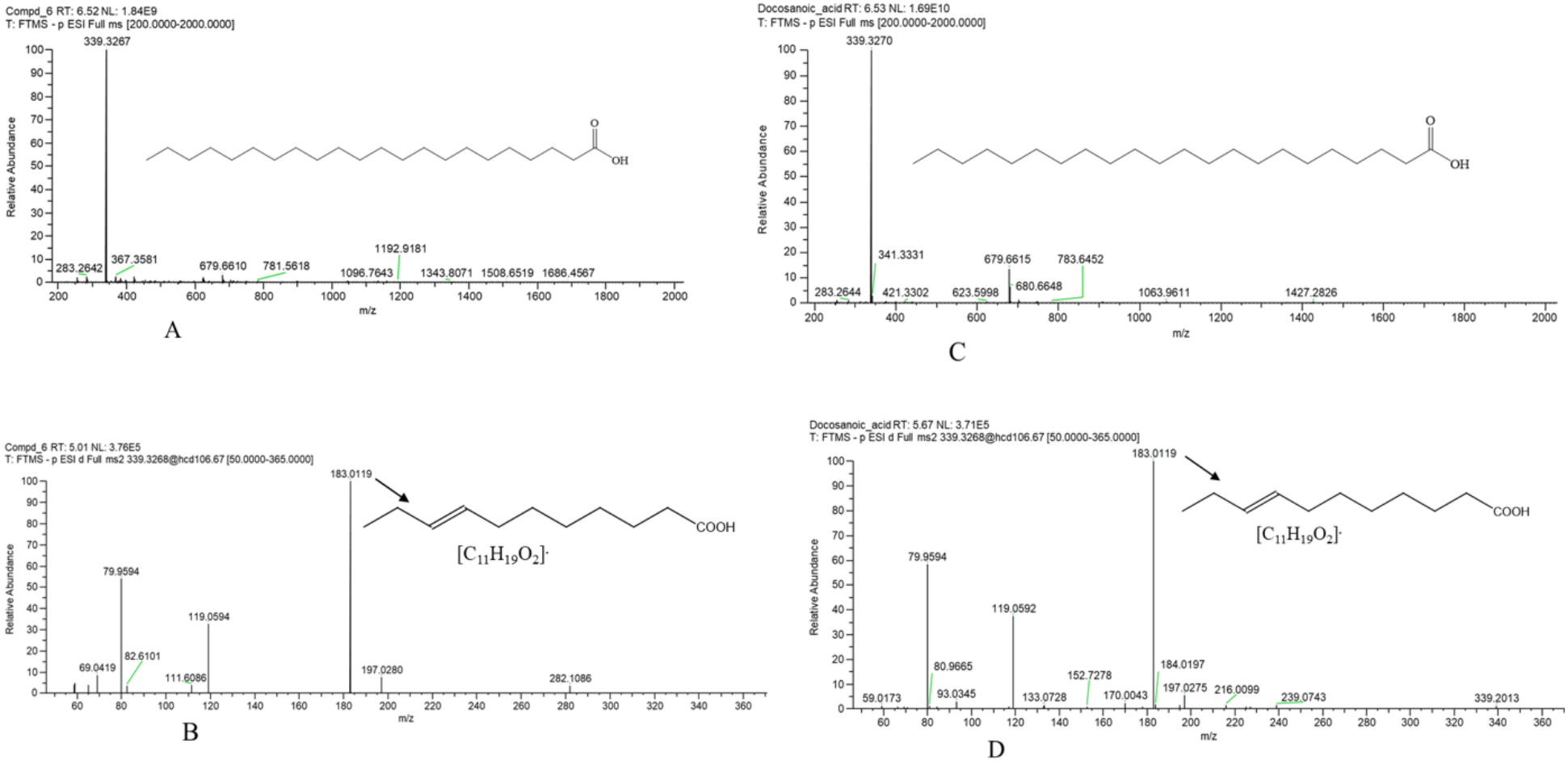

Figure 8b: Full scan and MS/MS of spot 6 (A-B) and authentic standard, docosanoic acid (C-D) showing molecular ion peak and characteristic fragments

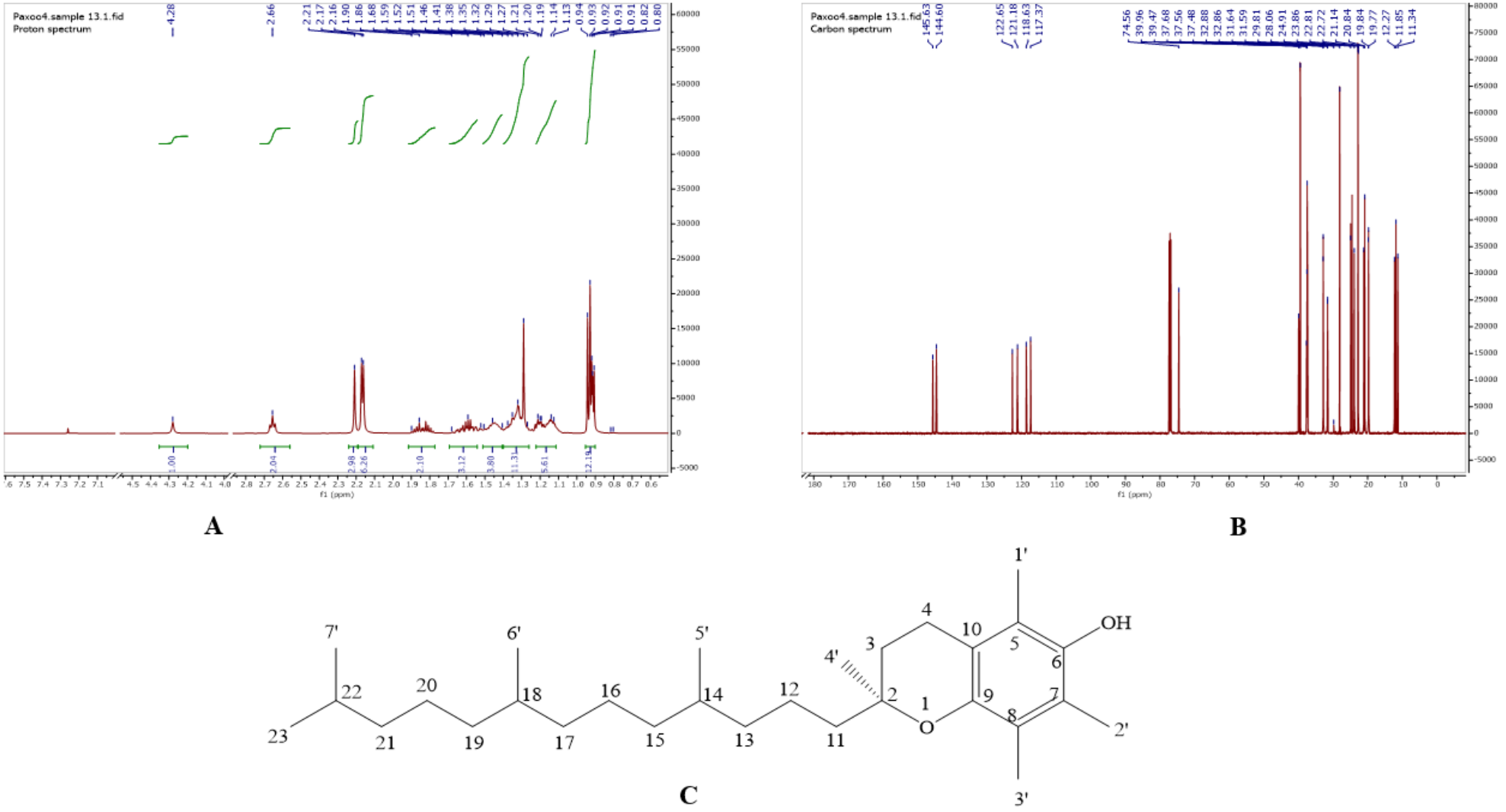

Figure 9a: ^{1}H NMR (A), ^{13}C NMR (B) spectra and chemical structure of compound 13 (α-tocopherol, $C_{29}H_{50}O_2$) (C) isolated from *M. cecropioides* leaf extract.

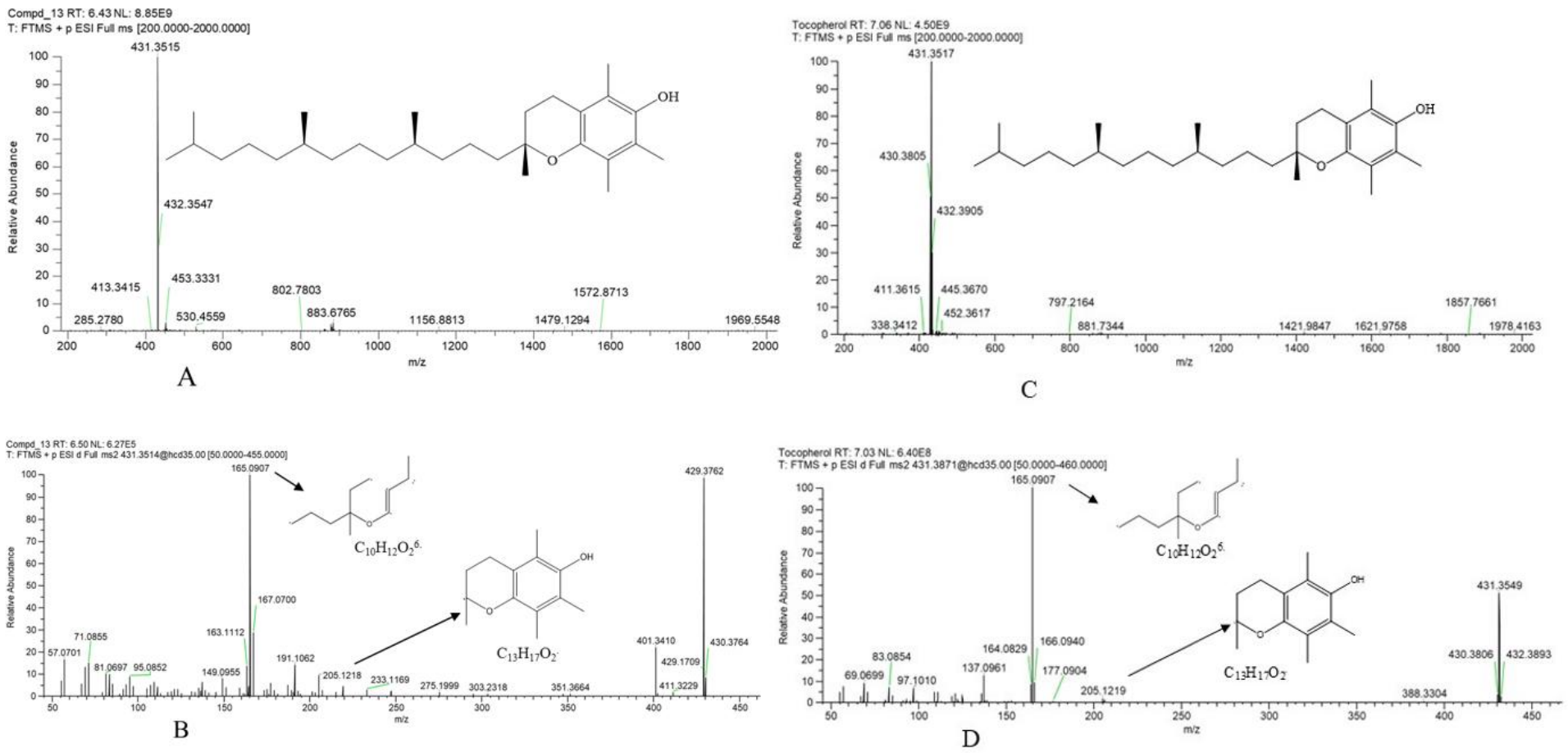

Figure 9b: Full scan and MS/MS of compound 13 (A-B) and authentic standard, α-tocopherol (C-D) showing molecular ion peak and characteristic fragments

There is growing evidence indicating both beneficial and detrimental effects of reactive oxygen species (ROS) on cancer cells. At low to moderate levels, ROS operate as regulators of important signalling pathways activating cancer cell proliferation, and migration and contributing to cell survival. In contrast, high levels of ROS are detrimental to cancer cells as they damage DNA, proteins, and lipids and eventually leading to cell death [21,22]. ROS plays crucial role in apoptotic cell death through the activation of several protease families, the most prominent being caspases [23]. Given the apoptosis and caspase results, to further investigate the possibility that ROS acted as initiators in MCL extract-induced apoptosis in breast cancer cells, the effect of MCL extract on levels of H_20_2 was measured in MCF-7 and MDA-MB-231 cells following 24 h treatment at a concentration of 1 x GI_{50}. In MCF-7 cells, MCL extract treatment led to a significant increase ($p<0.001$) in H_20_2 levels to 141.29±3.03% of control comparable with etoposide ($p<0.0001$) (151.89±9.65%) (Figure 6 A). Furthermore, in MDA-MB-231 cells the extract also exhibited a significant increase ($p<0.05$) in H_20_2 levels to 115.20±6.25% of control (Figure 6 B).

Phosphorylation of the H2AX protein (γ-H2AX) is an early stage in the double-strand break (DSB) repair process and is often employed as a marker of DNA DSBs [24] . To further understand the mechanism behind the cytotoxicity displayed by MCL extract, the percentage of phosphorylated histone H2AX which resulted in double-strand breaks to form γ-H2AX positive cells was assessed. The assessment of DNA damage following treatment with MCL extract was conducted by quantifying the percentage of cells expressing γ-H2AX through flow cytometric techniques. As demonstrated in Figure 7a, MCL extract significantly ($p<0.05$, $p<0.01$ and $p<0.0001$) increased the formation of γ-H2AX in MCF-7 cells by ~2.9, ~4.5 and ~6.6-fold relative to control after 24 h exposure period at 0.5 x GI_{50}, 1 x GI_{50} and 2 x GI_{50}, respectively. In MDA-MB-231 cells, the extract also caused a significant dose-dependent elevation of γ-H2AX ($p<0.001$ and $p<0.0001$) after 24 h treatment at 0.5 x GI_{50}, 1 x GI_{50} and 2 x GI_{50} by ~2.5, ~8.2 and ~11.9-fold respectively, relative to control (Figure 7b). Supplementary file Figures S5 and S6 also show representative dot plot of γ-H2AX -expressing cells in both cell lines treated with MCL extract.

Based on the results from the cytotoxicity studies, the crude ethanol extract of MCL was subjected to fractionation using solvents of increasing polarity including n-hexane, dichloromethane (DCM), ethyl acetate (EA), butanol (BuOH) through liquid-liquid chromatographic separation. Supplementary file Figure S7 shows the schematic diagram of the fractionation of MCL crude extract. Fractions obtained were hexane (32.18 g), DCM (35.85 g), ethyl acetate (22.39 g), butanol (35.13 g) and aqueous (51.14 g). The growth-inhibitory activity of the fractions was determined by MTT assay. The fractions were tested against MCF-7 cells because the crude extract showed higher selectivity towards the cancer cell line. From the results, the DCM fraction exhibited the highest growth-inhibitory effect against MCF-7 cells with a GI_{50} concentration of 2.02 µg/mL. Similarly, ethyl acetate also exhibited significant growth-inhibitory effect (GI_{50} concentration = 2.68 µg/mL). The extent of antiproliferative activity was in the order: dichloromethane>ethyl acetate> hexane>butanol> aqueous. Table 1 summarises the results.

The DCM and ethyl acetate fractions of MCL extract which showed profound growth-inhibitory activities were further purified using column chromatography, thin-layer chromatography, and preparative thin-layer chromatography (prep TLC). The DCM fraction (34 g) was separated using silica gel on column chromatography and eluted with solvent gradients of hexane: ethyl acetate (100:0 and 0:100) and ethyl acetate: methanol (100:0 and 0:100) to give subfractions. Six fractions (fractions D1-D6) were obtained from this separation after pooling fractions with similar chromatographic profiles and retention time together. Sub-fractions D1, D2, D3, D4 and D6 were subjected to further purification steps using hexane: ethyl acetate gradients and thin-layer chromatography was used to monitor the separation after which fractions with similar profiles were combined. After repeated chromatographic separations, sub-fractions D1.1, D2.1. D2.2, D3.2, D4.1, D4.2, D6.1 and D6.2 were re-chromatographed using prep TLC at different ratios of hexane: ethyl acetate to give spots 1 to 17 (supplementary file Figure S8). The ethyl acetate fraction (19 g) was separated using silica gel on column chromatography and eluted with solvent gradients of hexane: ethyl acetate (100:0 and 0:100) and ethyl acetate: methanol (100:0 and 0:100) to give 5 subfractions obtained after combining fractions based on thin-layer chromatography profiles. Sub-fractions E1, E2 and E3, were subjected to further purification steps using hexane: ethyl acetate gradients and monitoring with thin-layer chromatography. After a series of chromatographic separations sub-fractions E1.1, E1.2 E2.1, E2.2, and E3.1 were re-chromatographed using preparative thin-layer chromatography at ratios of hexane: ethyl acetate to give spots 18 to 28 (supplementary file Figure S10).

Spot 6 (12.1 mg): C22H44O2, yellowish oil, Rf = 0.75. IR (CDCl3, ATR, cm-1) = 1800 (C=O), 2920 (CH2), 2840 (-CH3) (supplementary file Figure S9). 1H-NMR (500 MHz, CDCl3): δH 2.35 (2H, t, H-2), 1.60 (2H, m, H-3), 1.25 (36H, m, H-4 to H-21), 0.89 (3H, t, H-22) (Figure 8a (A)). HSQC (500 MHz, CDCl3): 0.90, 14.16 (C-22), 1.31, 33.49 (C-21); 1.28, 32.19 (C-4 to C-19); 2.37, 34.23 (C-2); 1.28, 29.67 (C-20) and 1.65, 24.95 (C-3) (Figure 8a (B)). HRESI-MS m/z = 339.3267 [M-H]- (Calculated for C22H44O2-, [M-H]-, m/z = 339.3269), mass error < 5 ppm. Spot 6 was identified as docosanoic acid, IUPAC name: Docosanoic acid (Figure 8a (C)) after comparing with the spectral data of authentic reference standard and literatures (Figure 8b (A-D) and supplementary file Figure S11 - S12).

Spot 13 (14.1 mg): $C_{29}H_{50}O_2$, colourless oil, Rf = 0.31. IR ($CDCl_3$, ATR, cm^{-1}) = 3200 (-OH), 2920 (CH_2), 2840 ($-CH_3$) and 1450 (phenyl skeletal bending) (supplementary file Figure S13). ^{1}H-NMR (500 MHz, $CDCl_3$,): δ_H 4.28 (1H, s, 6-OH), 2.66 (2H, t, H-4), 2.21 (3H, s, H-1'), 2.17 (3H, s, H-2'), 2.16 (3H, s, H-3'), 1.90-1.86 (2H, q, H-3), 1.68-1.52 (3H, m, H-11, H-12, H-14), 1.51- 1.41 (4H, m, H-13, H-15, H-22), 1.38-1.27 (11H, m, H-18, H-16, H-21, H-20), 1.23-1.13 (6H, m, H-19, H-17, H-4'), 0.94-0.91 (12H, m, H-5', H-6', H-7', H-23) (Figure 19a (A)). ^{13}C-NMR (500 MHz, $CDCl_3$,): δ_C 145.6 (C-9), 144.6 (C-6), 122.7 (C-8), 121.2 (C-7), 121.2 (C-7), 118.6 (C-5), 117.4 (C-10), 74.6 (C-2), 40.0 (C-11), 39.5 (C-21), 37.7 (C-13), 37.6 (C-15), 37.5 (C-17), 32.9 (C-19), 32.9 (C-14), 31.6 (C-18), 31.6 (C-3), 29.8 (C-21), 28.06 (C-16), 24.9 (C-20), 23.9 (C- 4'), 22.8 (C-7'), 22.7 (C-23), 21.1 (C-12), 20.8 (C-4), 19.8 (C-5'), 19.8 (C- 6'), 12.3 (C- 2'), 11.9 (C- 3'), 11.3 (C- 1') (Figure 9a (B)). HRESI-MS m/z = 431.3515 $[M+H]^+$ (calculated for $C_{29}H_{50}O_2^+$, $[M+H]^+$, 431.3889), mass error < 5ppm. Spot 13 was identified as α-tocopherol (Figure 9a (C)) after comparing with the spectral data of authentic reference standard and literatures (Figure 9b (A-D) and supplementary file Figure S14 - S15).

DISCUSSION

In this study, the mechanism by which *Musanga cecropioides* leaf extract (MCL) exerts growth-inhibitory effects on MCF-7 and MDA-MB-231 cells was explored. In addition, the bioactive components in MCL were analysed by IR spectroscopy, NMR, and LC-HRESI/MS to determine the relationship between the anticancer potential and chemical composition. The cell viability assay revealed that the extract inhibited the proliferation of MCF-7 and MDA-MB-231 cells in a concentration-dependent manner with the extract showing greater selectivity towards the cancer cells compared with the non-cancer cells, (MRC-5). Malignancies develop as a result of mutations that enable cells to advance through the cell cycle while evading certain checkpoints [25] Findings from this study suggest that inhibition of cell proliferation by MCL extract may be linked to G1 phase arrest in MCF-7 cells and possibly G2/M phase arrest in MDA-MB-231 cells. The possibility of G2/M phase arrest in MDA-MB-231 by MCL

extract correlates with previous reports of other researchers where *Bryonia dioica* extract induced G2/M phase in MDA-MB-231 cells [26] The G1 phase cell arrest of MCF-7 cells by MCL extract is consistent with the report of other researchers where the extract of *Vernonia amygdalina* induced G1 phase arrest in MCF-7 cells but not in MDA-MB-231 cells [27]. Cell arrest of MCF-7 cells by MCL extract during the G1 phase suggests that the extract disrupts cell progression from G1 to S-phase and suggests that the inhibition of MDA-MB-231 cell growth could be associated with G2/M phase cell cycle arrest. In the two breast cancer cell lines, compared with control, a significant G2/M phase accumulation in a time-dependent manner was produced by etoposide (positive control). This also suggests that the mechanism of action of MCL extract in MCF-7 cells could be different from that of etoposide but could be the same in MDA-MB-231 cells. Elucidating the mechanism of action of MCL extract revealed that it caused perturbation in cell cycle progression evident by the G1 phase arrest in MCF-7 and possibly G2/M phase arrest in MDA-MB-231 cells. Taken together, cell cycle arrest is thought to be one of the mechanisms by which MCL extract exerts its anticancer activity in these two cell lines.

Apoptosis, or programmed cell death, is tightly regulated at the gene level, resulting in the orderly and effective clearance of damaged cells such as those that occur after DNA damage or during development [28]. Deregulation of this death mechanism has been linked to unregulated cell proliferation, cancer growth and progression, and resistance to therapeutic therapy [29]. It is well known that inducing apoptosis is a potentially effective cancer treatment method [30]. Investigating the apoptosis-inducing potential of the extract in both MCF-7 and MDA-MB-231 cells revealed that in MCF-7 cells, the extract exhibited a significant increase in early and late apoptotic cell populations particularly at lower concentrations and at short duration of treatment. However, at longer treatment periods, late apoptotic cell populations increased, gearing towards necrosis. Similarly, in MDA-MB-231 cells, the extract displayed a late apoptotic effect at all treatment periods and concentrations which was also accompanied by significant increase in necrotic cell populations. The result from this investigation indicates that the cytotoxic activities displayed by MCL extract could be attributed to apoptotic and necrotic forms of cell death which is in line with the findings of [31] who showed that *Juniperus phoenicea* mediated inhibition of MCF-7 cells through apoptosis as well as necrosis induction. Moreover, it is becoming more widely recognized that conventional chemotherapeutic agents also cause various forms of cell death including necrosis, autophagy, mitotic catastrophe, and senescence in addition to apoptosis [32].

Concerning the effect of the extract on caspase 3/7 activity on the two breast cancer cells, A profound increase in caspase 3/7 activity was observed in MDA-MB-231 cells which suggested the involvement of caspases in apoptosis induction in MDA-MB-231 cells. This effect was however not significant in MCF-7 cells, possibly due to lack of functioning caspase-3 in MCF-7 cells due to a 47-base loss within exon 3 of the CASP-3 gene [33], thus indicating the unlikely involvement of caspases in the apoptosis-inducing potential of the extract in MCF-7 cells. This results also implies that caspases play an important role in the induction of apoptosis by MCL extract in MDA-MB-231 cells.

Excessive ROS production or failure of oxidant scavenging mechanisms can disrupt cellular function by inducing the oxidation of lipids, proteins, and DNA [34]. The level of H_20_2 produced following treatment with the extract was significantly higher than the control in both breast cancer cells. Taken together, the ability of MCL extract to elevate ROS production in MCF-7 cells and MDA-MB-231 could be one of the mechanisms through which the extract exerts its anticancer potential. This result aligns with other studies where the cytotoxicity exhibited by the extract of *Galenia africana* in breast cancer cells (MCF-7 and MDA-MB-231) is thought to be via ROS-mediated cell death [35].

Evidence of double-strand DNA breaks (DSBs) in MCF-7 and MDA-MB-231-treated cells was investigated by measuring phosphorylated γ-H2AX levels. In the two cells, the extract caused significant dose-dependent increase in cells expressing γ-H2AX which is indicative of DNA DSBs. This result suggests that the induction of DNA DSBs in MCF-7 and MDA-MB-231 cells could be a possible mechanism by which the extract exhibits its cytotoxicity. These results are consistent with other studies where *Ginkgo biloba* leaf extract induced DNA damage in HepG2 cells by demonstrating a concentration- and time-dependent increase in γ-H2AX positive cells [36]. Furthermore, in relation to the ROS results, it is likely that DNA damage in the two breast cancer cell lines is a direct consequence of ROS produced in the extract-treated cells as other studies have also reported ROS-induced DNA damage in cells following treatment with some natural products such as curcumin [37]. Therefore, the possibility of MCL extract inducing DNA damage by mechanisms dependent of ROS cannot be ruled out. Overall, the mechanistic assessments suggests that the induction of apoptosis in the two breast cancer cell lines by MCL extract could be related to the generation of ROS as well induction of DNA DSBs.

Fractionation of crude MCL extract afforded five fractions of hexane, dichloromethane (DCM), ethyl acetate (EA), butanol and water (AQ). Growth-inhibitory activity of the fractions determined via MTT assay revealed that the bioactive components with cytotoxic potential were concentrated in the DCM (GI_{50} concentration = 2.02 µg/mL) and ethyl acetate (GI_{50} concentration = 2.68 µg/mL) fractions. Further series of purification of these two most active fractions afforded 28 spots.

A combination of all generated spectroscopic data facilitated the identification of spot 6 as docosanoic acid. This identity is also in agreement with those in spectral libraries and published articles [38,39]. Docosanoic acid is a long-chain saturated fatty acid also known as behenic acid consisting of at least 22 carbon atoms with a molecular formula of $C_{22}H_{44}O_2$. It is a naturally occurring compound that has also been isolated from other medicinal plants including the aerial part of *Lantana camara* [40], flowers of *Cercis chinensis* [41], and also from the root of *Millettia speciosa* [42]. This is the first report of its isolation from the leaves of *Musanga ceropioides* extract.

While minor differences were observed in the absorption spectra between Spot 13 and the α-tocopherol standard, particularly in the 3600–2800 cm^{-1} and 3200–2400 cm^{-1} regions, these could be attributed to sample concentration differences and corresponded to asymmetric and symmetric CH_2/CH_3 stretching vibrations. These findings align with prior infrared spectroscopic studies on α-tocopherol [43,44]. ^1H NMR and ^{13}C NMR analysis of spot 13 identified 50 protons and 29 carbons, respectively, supported by DEPT-135 spectra. The data indicated six aromatic quaternary carbons, two oxygenated carbons (δ = 144.6 and 145.6 ppm), three methylated carbons (δ = 118.5, 121.2, 122.6 ppm), and a combination of methine, methylene, and methyl carbons consistent with the α-tocopherol structure [45]. HRESI-MS further confirmed the compound with a molecular ion peak at m/z 431.3515 $[M+H]^+$ and a fragment at m/z 165.0907, analytically similar to the authentic sample (m/z 431.3517). Taken together, the IR, NMR, and MS data confirmed the identity of Spot 13 as α-tocopherol, supported by comparisons with an authentic standard under the same analytical conditions, spectral libraries, and previous studies.

The ^1H NMR data obtained for compound 13 revealed the saturated phytyl chain and HRESI-MS and MS/MS data facilitated the identification to be α-tocopherol as different from the rest of the tocopherols or tocotrienols. α-tocopherol has been isolated from the bulb of garlic, *Allium sativum* [46], wheat germ oil [47], fruit peels of *Fortunella japonicum* [45], and *Jatropha tanjorensis* leaves [48] but this is the first report of its isolation from *Musanga cecropioides* leaf extract.

Some compounds have been isolated from the different parts of *Musanga cecropioides* plant, they include tormentic acid, 2-acetyl

tormentic acid, 3-acetyl tormentic acid, euscaphic acid, three seco-triacidic triterpenes, cecropic acid methyl ester, cecropiacic acid, musangic acids A and B, musangicic acid from the rootwood [49–52]. Also, kalaic acid, protocatechuic acid and protocatechualdehyde have been isolated from the stembark (53,54). This study has revealed the isolation of two known compounds including docosanoic acid (spot 6) and α-tocopherol (spot 13) from the leaves of this plant for the first time.

CONCLUSION

The result from this study reveals that *Musanga cecropioides* leaf extract exhibits significant anticancer activity against MCF-7 and MDA-MB 231 cancer cell lines through mechanisms including cell cycle arrest, apoptosis induction, ROS generation and DNA DSBs induction.

Acknowledgments

The authors greatly appreciate the University of Lagos and the Tertiary Education Trust Fund (TETFUND, Nigerian Government) for the scholarship awarded to OOO. The support of Dr Sandra Martinez Jarquin of the Centre for Analytical Biosciences (CAB), University of Nottingham who assisted in interpreting and analysing the LC-MS data is also well appreciated.

Conflict of interest

The authors declared no conflict of interest.

Financial Support

None declared.

ORCID ID

Olubusola Omobolanle Olaleye: https://orcid.org/0000-0003-1145-2558

Dong-Hyun Kim: https://orcid.org/0000-0002-3689-2130

Keith A Spriggs: https://orcid.org/0000-0001-5946-1440

Supplementary materials

Supplementary material associated with this article can be found in the online version, at:

https://phytopharmajournal.com/Vol14_Issue3_10_supplementary.pdf

REFERENCES

1. Bray F, Ferlay J, Soerjomataram I, Siegel RL, Torre LA, Jemal A. Global cancer statistics 2018: GLOBOCAN estimates of incidence and mortality worldwide for 36 cancers in 185 countries. CA Cancer J Clin. 2018;68(6):394–424.
2. Debela DT, Muzazu SGY, Heraro KD, Ndalama MT, Mesele BW, Haile DC, et al. New approaches and procedures for cancer treatment: Current perspectives. SAGE Open Med. 2021;9.
3. Hossan MS, Break MK Bin, Bradshaw TD, Collins HM, Wiart C, Khoo TJ, et al. Novel semi-synthetic cu (Ii)–cardamonin complex exerts potent anticancer activity against triple-negative breast and pancreatic cancer cells via inhibition of the akt signaling pathway. Molecules. 2021;26(8).
4. Rathor L. Medicinal Plants: A Rich Source of Bioactive Molecules Used in Drug Development. In: Mandal SC, Chakraborty R, Sen S, editors. Evidence Based Validation of Traditional Medicines: A comprehensive Approach. Singapore: Springer Singapore; 2021. p. 195–209.
5. Dike IP, Obembe O. Towards conservation of Nigerian medicinal plants. J Med Plants Res. 2012;6:3517–21.
6. Sufian AS, Ramasamy K, Ahmat N, Zakaria ZA, Yusof MIM. Isolation and identification of antibacterial and cytotoxic compounds from the leaves of *Muntingia calabura* L. J Ethnopharmacol. 2013;146(1):198–204.
7. Sasidharan S, Chen Y, Saravanan D, Sundram KM, Yoga Latha L. Extraction, isolation, characterization, of bioactive compounds from plants' extract. 2011;8(1):1–10.
8. Zhao CL, Chik WI, Zhang HJ. Chapter 22 - Bioprospecting and bioassay-guided isolation of medicinal plants—A tool for drug discovery. In: Mukherjee PK, editor. Evidence-Based Validation of Herbal Medicine (Second Edition). Second Edi. Elsevier; 2022. p. 511–37.
9. Ingle KP, Deshmukh AG, Padole DA, Dudhare MS, Moharil MP, Khelurkar VC. Phytochemicals: Extraction methods, identification and detection of bioactive compounds from plant extracts. J Pharmacogn Phytochem. 2017;6(1):32–6.
10. Santiago M, Strobel S. Thin layer chromatography. Methods Enzymol. 2013;533:303–24.
11. Rasul MG. Extraction, Isolation and Characterization of Natural Products from Medicinal Plants. International Journal of Basic Sciences and Applied Computing (IJBSAC). 2018;(6):2394–367.
12. Burkill HM. A revision of Dalziel's useful plants of west tropical Africa. Vol. 1. Kew, UK: Royal Botanical Gardens; 1985.
13. Burkill HM. The Useful Plants of West Tropical Africa. 2nd Edition, Volume 4 (Families M-R). 2nd Editio. Royal Botanic Gardens, Kew; 1997. 757 p.
14. Olaleye OO, Kim DH, Spriggs KA. Antiproliferative activities of some selected Nigerian medicinal plants against breast, liver, and cervical cancer cells. BMC Complement Med Ther. 2024;24(1):110.
15. Badmus JA, Ekpo OE, Hussein AA, Hiss MM and DC. Cytotoxic and cell cycle arrest properties of two steroidal alkaloids isolated from *Holarrhena floribunda* (G. Don) T. Durand & Schinz leaves. BMC Complement Altern Med. 2019;19:112.
16. Crowley LC, Marfell BJ, Scott AP, Waterhouse NJ. Quantitation of apoptosis and necrosis by annexin V binding, propidium iodide uptake, and flow cytometry. Cold Spring Harb Protoc. 2016;2016(11):953–7.
17. Break MK Bin, Hossan MS, Khoo Y, Qazzaz ME, Al-Hayali MZK, Chow SC, et al. Discovery of a highly active anticancer analogue of cardamonin that acts as an inducer of caspase-dependent apoptosis and modulator of the mTOR pathway. Fitoterapia. 2018;125(January):161–73.
18. Badmus JA, Ekpo OE, Hussein AA, Meyer M, Hiss DC. Antiproliferative and apoptosis induction potential of the methanolic leaf extract of *Holarrhena floribunda* (G. Don). Evidence-based Complementary and Alternative Medicine. 2015;2015.
19. Park J, Shin Y, Kim TH, Kim DH, Lee A. Plasma metabolites as possible biomarkers for diagnosis of breast cancer. PLoS One. 2019;14(12):1–12.
20. Ferlay J, Colombet M, Soerjomataram I, Parkin DM, Piñeros M, Znaor A, et al. Cancer statistics for the year 2020: An overview. Int J Cancer. 2021;149(4):778–89.
21. Moloney JN, Cotter TG. ROS signalling in the biology of cancer. Semin Cell Dev Biol. 2018;80:50–64.
22. Sabharwal SS, Schumacker PT. Mitochondrial ROS in cancer: initiators, amplifiers or an Achilles' heel? Nat Rev Cancer. 2014;14(11):709–21.
23. Perillo B, Di Donato M, Pezone A, Di Zazzo E, Giovannelli P, Galasso G, et al. ROS in cancer therapy: the bright side of the moon. Exp Mol Med. 2020;52(2):192–203.

24. Firsanov D V., Solovjeva L V., Svetlova MP. H2AX phosphorylation at the sites of DNA double-strand breaks in cultivated mammalian cells and tissues. Clin Epigenetics. 2011;2(2):283–97.
25. Lee H, Kim W, Kang HG, Kim WJ, Lee C, Kim SJ. Geranium thunbergii extract-induced G1 phase cell cycle arrest and apoptosis in gastric cancer cells. 2019;
26. Benarba B, Elmallah A, Pandiella A. Bryonia dioica aqueous extract induces apoptosis and G2/M cell cycle arrest in MDA-MB 231 breast cancer cells. Mol Med Rep. 2019;20(1):73–80.
27. Wong FC, Woo CC, Hsu A, Tan BKH. The Anti-Cancer Activities of *Vernonia amygdalina* Extract in Human Breast Cancer Cell Lines Are Mediated through Caspase-Dependent and p53-Independent Pathways. PLoS One. 2013;8(10).
28. Fuchs Y, Steller H. Programmed cell death in animal development and disease. Cell. 2011 Nov;147(4):742–58.
29. Plati J, Bucur O, Khosravi-Far R. Dysregulation of apoptotic signaling in cancer: molecular mechanisms and therapeutic opportunities. J Cell Biochem. 2008 Jul;104(4):1124–49.
30. Schulze-Bergkamen H, Krammer PH. Apoptosis in cancer--implications for therapy. Semin Oncol. 2004 Feb;31(1):90–119.
31. Barnawi IO, Nasr FA, Noman OM, Alqahtani AS, Al-Zharani M, Alotaibi AA, et al. Induction of apoptosis and cell cycle arrest by chloroform fraction of *Juniperus phoenicea* and chemical constituents analysis. Open Chem. 2021;19(1):119–27.
32. Ricci MS, Zong WX. Chemotherapeutic Approaches for Targeting Cell Death Pathways. Oncologist. 2006;11(4):342–57.
33. Groth-Pedersen L, Ostenfeld MS, Høyer-Hansen M, Nylandsted J, Jäättelä M. Vincristine induces dramatic lysosomal changes and sensitizes cancer cells to lysosome-destabilizing siramesine. Cancer Res. 2007;67(5):2217–25.
34. Murphy MP, Holmgren A, Larsson NG, Halliwell B, Chang CJ, Kalyanaraman B, et al. Unraveling the biological roles of reactive oxygen species. Cell Metab. 2011 Apr;13(4):361–6.
35. Mohamed L, Chakraborty S, ArulJothi KN, Mabasa L, Sayah K, Costa-Lotufo L V., et al. Galenia africana plant extract exhibits cytotoxicity in breast cancer cells by inducing multiple programmed cell death pathways. Saudi Pharmaceutical Journal. 2020;28(10):1155–65.
36. Zhang Z, Chen S, Mei H, Xuan J, Guo X, Couch L, et al. Ginkgo biloba leaf extract induces DNA damage by inhibiting topoisomerase II activity in human hepatic cells. Sci Rep. 2015;5(April):1–13.
37. Thayyullathil F, Chathoth S, Hago A, Patel M, Galadari S. Rapid reactive oxygen species (ROS) generation induced by curcumin leads to caspase-dependent and -independent apoptosis in L929 cells. Free Radic Biol Med. 2008;45(10):1403–12.
38. Sleighter RL, Mckee GA, Liu Z, Hatcher PG. Naturally present fatty acids as internal calibrants for fourier transform mass spectra of dissolved organic matter. Limnol Oceanogr Methods. 2008;6(6):246–53.
39. Xie Y, Peng Q, Ji Y, Xie A, Yang L, Mu S, et al. Isolation and Identification of Antibacterial Bioactive Compounds From *Bacillus megaterium* L2. Front Microbiol. 2021;12(March):1–10.
40. Ayub A, Begum S, Ali SN, Ali ST, Siddiqui BS. Triterpenoids from the aerial parts of *Lantana camara*. J Asian Nat Prod Res. 2019;21(2):141–9.
41. Zhang J, Zhou L, Cui L, Liu Z, Wei J, Kang W. Antioxidant and α-glucosidase inhibitiory activity of Cercis chinensis flowers. Food Science and Human Wellness. 2020;9(4):313–9.
42. Ding P, Qiu J ying, Ge Y, Dai L. Chinese Herbal Medicines (CHM) Letter Chemical Constituents from Barks of *Lannea coromandelica*. Chin Herb Med. 2014;6(1):65–9.
43. Silva SD, Rosa NF, Ferreira AE, Boas L V., Bronze MR. Rapid determination of α-tocopherol in vegetable oils by fourier transform infrared spectroscopy. Food Anal Methods. 2009;2(2):120–7.
44. Che Man YB, Ammawath W, Mirghani MES. Determining α-tocopherol in refined bleached and deodorized palm olein by Fourier transform infrared spectroscopy. Food Chem. 2005;90(1–2):323–7.
45. Jeong-Yong C, Kazuyoshi K, Jae-Hak M, Keun-Hyung P, Kotaro M, Yoshihisa T. Chemical Constituents from tile Fruit Peels of *Fortunella japonica*. Food Sci Biotechnol. 2005;14(5):599–603.
46. Malik MN, Fenko MD, Shiekh AM, Wisniewski HM. Isolation of α-Tocopherol (Vitamin E) from Garlic. J Agric Food Chem. 1997;45(3):817–9.
47. Evans HM, Emerson OH, Emerson GA. The Isolation from Wheat Germ Oil of an Alcohol, α-Tocopherol, Having the Properties of Vitamin E. Nutr Rev. 1974;32(3):80–2.
48. Ijoma KI, Ajiwe VIE. Jatropha tanjorensis a Flora of Southeast Nigeria: Isolation and Characterization of Naringenin and Validation of Bio-enhanced Synergistical Activity of α-Tocopherol Toward Clinical Isolates of Resistant Bacterial. Makara J Sci. 2022;26(2):120–7.
49. Lontsi D, Sondengam BL, Martin MT, Bodo B. Seco-ring-A-triterpenoids from the rootwood of *Musanga cecropioides*. Phytochemistry. 1991;30(5):1621–4.
50. Ojinnaka CM, Okogun JI. Millbank, London: Crown Agents for Overseas Government and Administrators. Vol. 24, Arch. Pharm. (Athens). Cambridge: University Press; 1968.
51. Lontsi D, Sondengam BL, Martin MT, Bodo B. Musangicic acid, a triterpenoid constituent of *Musanga cecropioides*. Phytochemistry. 1992;31(12):4285–8.
52. Lontsi D, Sondengam BL, Ayafor JF, Tsoupras MG, Tabacchi R. Further triterpenoids of *Musanga cecropioides*: The structure of cecropic acid. Planta Med. 1990;56(3):287–9.
53. Ayinde BA, Onwukaemea, D. N. Omogbai EK. Ayinde B. A., Onwukaemea D. N. and Omogbai E. K. (2007). Isolation and characterization of two phenolic compounds from the stem bark of *Musanga cecropioides* R. Brown (Moraceae). Acta Poloniae Pharmaceutica -Drug Research, 64(2): 183-185 Ayitey-Smith. Acta Poloniae Pharmaceutica -Drug Research. 2007;64(2):183–5.
54. Lontsi D, Sondengam BL, Bodo B, Martin MT. Kalaic acid, a new ursane-type saponin from *Musanga cecropioides*. Planta Med. 1998;64(2):189–91.

HOW TO CITE THIS ARTICLE

Olaleye OO, Kim DH, Spriggs KA. Evaluation of anticancer activity and phytochemical characterisation of *Musanga cecropioides* R. Br. ex Tedlie (Urticaceae) leaf extract. J Phytopharmacol 2025; 14(3):188-202. doi: 10.31254/phyto.2025.14310